Monte Carlo Evaluation Of Non-Linear Scattering Equations For Subsurface Reflection

Matt Pharr Pat Hanrahan

Stanford University

Abstract

We describe a new mathematical framework for solving a wide variety of rendering problems based on a non-linear integral scattering equation. This framework treats the scattering functions of complex aggregate objects as first-class rendering primitives; these scattering functions accurately account for all scattering events inside them. We also describe new techniques for computing scattering functions from the composition of scattering objects. We demonstrate that solution techniques based on this new approach can be more efficient than previous techniques based on radiance transport and the equation of transfer and we apply these techniques to a number of problems in rendering scattering from complex surfaces.

CR Categories: I.3.7 [Computer Graphics]: Three-Dimensional Graphics and Realism—Color, shading, shadowing, and texture; I.3.3 [Computer Graphics]: Picture/Image Generation

Keywords: Rendering, Illumination, Monte Carlo Techniques, Reflectance and Shading Models, Scattering Function, Invariant Imbedding, Principles of Invariance, Equation of Transfer, Adding Equations, Chandrasehkar's Equation

1 Introduction

In this paper we describe a new framework for solving a broad class of rendering problems. It consists of a non-linear integral *scattering equation* that describes the overall scattering behavior of an object or volume accounting for all of the scattering events that happen inside of it, and a set of *adding equations* that describe aggregate scattering functions from the composition of objects with known scattering functions.[1] In some situations, techniques based on these equations can be much more efficient than corresponding techniques based on the equation of transfer [Cha60] (*i.e.* the rendering equation [Kaj86]).

Unlike the equation of transfer, these equations describe the scattering from an object directly; thus they reflect a shift in focus from energy transport to scattering behavior independent of a particular illumination setting. This approach has been developed over the past fifty years, primarily in astrophysics, where these equations are often used to compute light scattering [Amb42, Cha60, van80]. In this paper, we will focus on their application to computing subsurface scattering.

The resulting scattering functions generalize the concept of the bidirectional reflectance distribution function (BRDF). The BRDF is based on the simplifying assumption that light exits the surface at the same point it enters, or equivalently that the surface is homogeneous and uniformly illuminated over a reasonably large area [NRH$^+$77]. This reduces the reflection function to a four-dimensional function over pairs of angles. BRDFs are the one-dimensional case since the surface may be inhomogeneous in the z dimension (the direction along the surface normal), but not in x and y.

More generally, Nicodemus *et al.* have introduced the bidirectional subsurface reflectance distribution function (BSSRDF) which accounts for light entering the surface at a different place than it exits [NRH$^+$77]. This is a three-dimensional scattering function that accounts for inhomogeneity in all dimensions underneath the surface; it gives reflectance along an outgoing ray due to illumination along an incoming ray. A minor generalization lifts the restriction to a planar surface, giving a scattering function of ten dimensions: five to specify the origin and direction of each ray. This setting lets us treat mathematically the scattering functions of general three-dimensional objects. The BRDF and BSSRDF are both important abstractions in that they describe scattering behavior phenomenologically such that lower-level scattering processes can be ignored.

Max *et al.* were the first graphics researchers to recognize the importance of the scattering equations [MMKW97]. They used the one-dimensional scattering equation to compute light scattering in tree canopies by deriving a system of ordinary differential equations. They solved this system with an adaptive Runge-Kutta method, using a clever application of the Fourier transform to avoid an $O(n^3)$ matrix multiplication. Because their solution technique discretizes the hemisphere into sets of angles, it becomes increasingly expensive for strongly peaked phase functions. More importantly, the viability of the extension of this solution method to 3D scattering problems has not been demonstrated. We develop the scattering equation in a more general setting that makes it possible to derive both one and three-dimensional scattering equations. We also derive and use the adding equations and apply a more general solution technique, Monte Carlo integration, that scales to the three-dimensional setting.

In this paper, we discuss the history of these scattering equations and previous work in graphics that has used different techniques to compute generalized scattering functions. We derive the scattering equations in integral form in a very general setting and describe the derivation of the adding equations. Given this basis, we describe the use of Monte Carlo techniques to compute solutions to these equations, demonstrate their efficiency, and apply them to a number of problems in rendering light reflection from complex surfaces. We conclude with discussion and directions for future work.

[1] We will use the term *scattering function* to describe the generic light scattering behavior of a surface or object, and we will use the term *scattering equation* to describe our Equation 3.5, which is equal to the scattering function in the general three-dimensional case.

2 Background and previous work

2.1 History of the scattering and adding equations

In a classic paper from the nineteenth century, Stokes derived expressions for the amount of light reflected and transmitted from a stack of glass layers [Sto62]. He introduced the innovations that overall scattering could be computed directly in terms of the reflection and transmission functions of the individual layers, and that the reflection and transmission for two layers together could be computed based on the already-computed reflection and transmission functions of each one. This work was the intellectual basis for the development of general scattering equations over the last fifty years.

The scattering and adding equations were first derived as a new way to compute 1D scattering functions without using the equation of transfer. The first applications were to the *standard problem* in astrophysics: given a slab of thickness z with known optical properties that do not vary in x or y and assuming that parallel beams of radiation are incident from a direction ω', we wish to know how much radiation is reflected in the direction ω (Figure 1).

Building on the ideas that Stokes developed, Ambarzumian derived a non-linear integral equation that describes scattering from semi-infinite homogeneous isotropic atmospheres directly in terms of the low-level scattering properties of the layers of the atmosphere [Amb42, Amb58].[2] Chandrasekhar greatly extended Ambarzumian's results and derived a non-linear integro-differential scattering equation that describes scattering from finite anisotropic atmospheres [Cha60]. Bellman and Kalaba extended this work to include inhomogeneity in depth and were the first to derive the purely integral form of this equation for theoretical analysis of solutions to the scattering equation [BK56, BKP63]. These one-dimensional scattering equations have been applied to a variety of other areas, including neutron transport, radiative transfer, and hydrologic optics [Mob94].

Recently, Wang has derived a scattering equation in the three-dimensional case where incident illumination from a distant source is constant over the entire upper boundary of the region and where the phase function varies only in z [Wan90] [NUW98, Section 4.6]. Unfortunately, this form is not generally useful for problems encountered in graphics.

The adding equations were developed by van De Hulst and Twomey *et al.* in the 1960s [van80, TJH66], and were later generalized by Preisendorfer [Pre76]. They were first discovered in the field of neutron transport by Peebles and Plesset [PP51] and have since been applied to a wide variety of scattering problems.

2.2 One-dimensional scattering functions

Computing scattering functions that hide the complexity of light scattering from surfaces has long been a research problem in graphics and optics. Examples include the Torrance–Sparrow reflection model [TS67], an analytic approximation to light scattering from rough surfaces; Blinn's model for dusty surfaces, which uses a single-scattering approximation [Bli82]; Kajiya's discussion of replacing complex geometry with reflection functions [Kaj85]; and Westin *et al.*'s computation of BRDF samples by simulating light scattering from micro-geometry [WAT92].

When no closed-form expression or approximation for multiple scattering at a surface is available, previous work has either ignored multiple scattering (*e.g.* [Bli82]), or based solutions on the equation of transfer and the definition of the BRDF (*e.g.* [WAT92]), where reflected radiance in the outgoing direction is computed given differential irradiance from the incident direction.

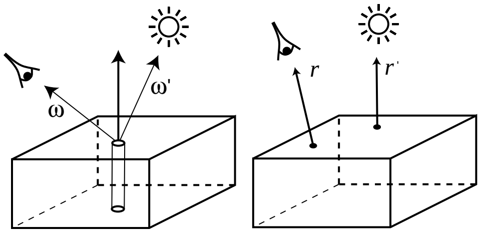

Figure 1: *Basic viewing geometry for the 1D (left) and 3D (right) scattering functions. All vectors and rays are specified in the outgoing direction.*

2.3 Three-dimensional scattering functions

In recent years, a number of researchers have worked on computing scattering functions that describe the aggregate scattering behavior of complex volumetric and geometric objects. Kajiya and Kay's volume texels were an early example [KK89], and Neyret extended their framework to include more general geometries and demonstrated applications to reducing aliasing due to level-of-detail changes [Ney98]. Rushmeier *et al.* approximated scattering from clusters of geometry by averaging the reflectance of surfaces hit by random rays [RPV93]. Sillion and Drettakis approximated occlusion due to complex objects as volume attenuation functions [SD95] and Sillion *et al.* approximated aggregate scattering functions from clusters of objects [SDS95]. However, none of these approaches accounts for multiple scattering inside the object or for light that enters the object at a different point than it exits.

Miller and Mondesir computed hypersprites that encoded specular reflection and refraction from objects [MM98], and Zongker *et al.* have described an apparatus for computing the scattering and transmission functions of glossy and specular real-world objects [ZWCS99]. Dorsey *et al.* have rendered rich images of stone and marble by computing BSSRDFs at rendering time [DEL$^+$99]. Their solutions are based on the equation of transfer and photon mapping to accelerate multiple scattering computations, and they clearly showed the importance of this effect for some materials. This is the only previous application in graphics of rendering scattering from surfaces with BSSRDFs.

In general, scattering from an object can be described by the formal solution of the inverse of the light transport equation [Pre65, Section 22]. Veach and Guibas derived rendering algorithms based on recursive expansion of this solution operator [VG94, Vea97] and Lafortune used the Neumann expansion of the solution operator to derive recursively-defined integral equations that describe scattering from a collection of surfaces; he called this the global reflectance distribution function (GRDF) and also used it to derive new light transport algorithms [LW94, Laf96].

2.4 Composing scatterers

A variety of techniques have previously been used to compute aggregate reflection functions from a set of layers. The Kubelka-Munk model [KM31] is similar to a one-dimensional radiosity solution; it accounts for multiple scattering but not angular dependence. It was first introduced to graphics by Haase and Meyer [HM92] and has been widely used. However, due to assumptions built into the model, either glossy specular reflection has to be ignored or multiple reflection between the specular component and the added layer is lost. A different approach to layer composition is due to Hanrahan and Krueger [HK93]; they compose scattering layers considering only one level of inter-reflection. This misses the effect of multiple internal reflections before light leaves the layer, which is important except for objects with very low albedos.

[2] Homogeneity refers to whether or not the atmosphere has scattering properties that vary as a function of depth, and isotropy refers to the properties of the phase function inside the atmosphere; an isotropic phase function scatters light equally in all directions.

x	Generic point
ω	Generic direction
r	A ray through space, with origin $x(r)$ and direction $\omega(r)$
μ_r	Cosine of ray's direction with surface normal
$\delta(x)$	Delta function: Kronecker or Dirac, depending on context
$\mathcal{S}^2$	The sphere of all directions
Ω	The hemisphere around the $+z$ direction
$\mathcal{M}^2$	A 2D manifold
$\mathcal{R}$	Ray space: a set of rays going through a set of locations in a set of directions
$\mathrm{L}(r)$	Radiance along the ray r
$\mathrm{p}(x, \omega' \to \omega)$	Phase function at a point.
$\mathrm{k}(r' \to r)$	Scattering kernel
$\mathrm{S}(r' \to r)$	Scattering function for light reflected along ray r due to incident light along ray r'
$\sigma_a(x)$	Volume absorption coefficient at x
$\sigma_s(x)$	Volume scattering coefficient
$\sigma_t(x)$	Volume attenuation coefficient, $\sigma_s(x) + \sigma_a(x)$
$\alpha(x)$	Albedo $\sigma_s(x)/\sigma_t(x)$
z	Depth in one-dimensional medium
$\mathrm{R}(z, \omega_i \to \omega_o)$	Reflection function from slab of depth z
$\mathrm{T}(z, \omega_i \to \omega_o)$	Transmission function from slab of depth z

Figure 2: *Table of notation.*

3 Scattering Equations

In this section, we derive the integral scattering equation that describes how an object or volume scatters light. We also describe techniques for computing the scattering functions of composite objects directly from the scattering functions of their constituent parts. Our treatment is in terms of the scattering of a single wavelength of light; the extension to multiple wavelengths is straightforward.

We will consider scattering from objects in an axis-aligned rectangular region of space with height z. This does not require that the object be parallelepiped-shaped; it is just a convenient parameterization of space. This parameterization also makes it possible to ignore the issue of non-convex regions of space, where illumination may exit and later re-enter the space. That setting is tractable, though the notation is more complex.

3.1 Ray space and operator notation

Previous work in graphics has used a variety of parameterizations of surfaces and directions for the expression of the rendering equation (*e.g.* Kajiya used an integral over pairs of points on surfaces). Veach has recently introduced abstractions based on *ray space* that have a number of advantages: in addition to simplifying and clarifying formulas, ray space makes clear that any particular parameterization of surfaces and directions is an arbitrary choice, mathematically equivalent to any other [VG95, Vea97].

In this setting, ray space $\mathcal{R}$ is the set of rays given by the Cartesian product of points in three-space $\mathbb{R}^3$ and all directions $\mathcal{S}^2$: $\mathcal{R} = \mathbb{R}^3 \times \mathcal{S}^2$. We will define two specializations of $\mathcal{R}$. First is $\mathcal{R}_{\mathcal{M}^2}$, which is the subset of $\mathcal{R}$ where all rays start on a given two-dimensional manifold $\mathcal{M}^2$: $\mathcal{R}_{\mathcal{M}^2} = \mathcal{M}^2 \times \mathcal{S}^2$. A particular instance of $\mathcal{R}_{\mathcal{M}^2}$ that is often useful is $\mathcal{R}_{\mathcal{M}^2(z')}$, where the manifold is the plane at $z = z'$. Another useful specialization is to limit the directions of rays $\mathcal{R}$ to the hemisphere around the surface normal; we denote this by $\mathcal{R}^+_{\mathcal{M}^2}$. The negation of a ray $-r$ is defined as the ray with the same origin as r but going in the opposite direction.

The scattering kernel k describes light scattering at a point. In ray space it is

$$\mathrm{k}(r' \to r) = \delta(x(r) - x(r'))\ \sigma_s(x(r))\ \mathrm{p}(x(r), \omega(r') \to \omega(r)),$$

where $\mathrm{p}(x(r), \omega(r') \to \omega(r))$ is the phase function at the point $x(r)$ for scattering from $\omega(r')$ to $\omega(r)$ and we have included the scattering coefficient σ_s in k in order to simplify subsequent formulas (see Chandrasekhar for a summary of phase functions, scattering coefficients, *etc*. [Cha60]).

In contrast to the phase function, the scattering function $\mathrm{S}(r' \to r)$ is potentially non-zero for any pair of rays because of multiple scattering; it is not necessary that the rays meet at a point for light along one ray to affect the response along another. Though the general scattering function is ten-dimensional, when we are considering scattering from a specific object, it is often more convenient to consider the eight-dimensional specialization where all rays originate on a parameterized two-dimensional manifold that bounds it. For the remainder of this paper, this is the only type of scattering function we will consider. In particular, we will just consider the scattering function from rays on a planar boundary of an object.

In order to be able to do integrals over $\mathcal{R}_{\mathcal{M}^2}$ and $\mathcal{R}_{\mathcal{M}^2(z)}$, we define a differential measure:

$$\mathrm{d}r = \mathrm{d}\omega(\omega(r))\,\mathrm{d}\mathrm{A}^{\perp}(x(r)) = \mu_r\,\mathrm{d}\omega(\omega(r))\,\mathrm{d}\mathrm{A}(x(r))$$

where $x(r)$ is the origin of r, $\omega(r)$ is its direction, A is the area measure on $\mathcal{R}_{\mathcal{M}^2}$, and $\mathrm{d}\omega$ is the differential solid angle measure.

Given an object's scattering function, outgoing radiance along a ray r is computed by integrating its product with incident radiance over the object's boundary.

$$\mathrm{L}_\mathrm{o}(r) = \frac{1}{4\pi} \int_{\mathcal{R}^+_{\mathcal{M}^2}} \frac{\mathrm{S}(r' \to r)}{\mu_r\,\mu_{r'}}\,\mathrm{L}_\mathrm{i}(r')\,\mathrm{d}r'$$

This is the three-dimensional analogue to integrating the product of incident radiance and the BRDF at a point to compute outgoing radiance. Its added complexity stems from the fact that incident light scatters inside the object and may exit far from where it entered.

We will define operators $\mathbf{k}$ and $\mathbf{S}$, where bold text signifies the operator and Roman text its kernel. Both operators are defined such that applying them to other functions gives:

$$(\mathbf{S}\,f)(r) = \int_{\mathcal{R}^+_{\mathcal{M}^2}} \frac{\mathrm{S}(r' \to r)}{\mu_r\,\mu_{r'}}\,f(r')\,\mathrm{d}r'$$

We can define compositions like $\mathbf{kS}$, or $\mathbf{S}_a\mathbf{S}_b\mathbf{S}_c$, *etc*. These will be useful in computing new scattering functions that describe the scattering of multiple objects in terms of their individual scattering functions (see Section 3.3).

$$(\mathbf{S}_1 \ldots \mathrm{S}_n)(r' \to r) = \int_{\mathcal{R}^+_{\mathcal{M}^2}} \cdots \int_{\mathcal{R}^+_{\mathcal{M}^2}} \mathrm{S}_n(r' \to r_1) \cdots \\ \mathrm{S}_1(r_{n-1} \to r)\,\frac{\mathrm{d}r_{n-1}}{\mu^2_{r_{n-1}}} \cdots \frac{\mathrm{d}r_1}{\mu^2_{r_1}} \qquad (3.1)$$

3.2 Derivation of the scattering equation

With operator notation in hand, we will derive a general integro-differential scattering equation in ray space. This equation describes how the scattering function of a complex object changes as layers with known scattering properties are added or removed from it. It can either be solved in integro-differential form or as a purely integral equation. Our derivation follows the *invariant imbedding* method [BK56, Pre58, BKP63, BW75].

We will consider the change in scattering behavior of this object as thin layers Δz are added on top of it. Because multiple scattering

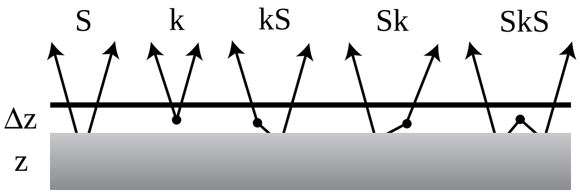

***Figure 3:** The five types of scattering events to be considered in the invariant imbedding derivation of the scattering equation. The S events reflect the aggregate multiple scattering inside the z slab. All other scattering events, such as* kSk*, are gathered in an* $o(\Delta z^2)$ *term in Equation 3.2.*

in Δz occurs with probability $o(\Delta z^2)$, we just gather all multiple scattering in an $o(\Delta z^2)$ term. Later we will divide by Δz and take the limit as $\Delta z \to 0$, at which point all of the $o(\Delta z^2)$ terms disappear. As such, there are only five types of scattering events that need to be accounted for (see Figure 3):

1. $\mathbf{S}$: Light that is attenuated in Δz, scattered by the original object, and attenuated again in Δz.
2. $\mathbf{k}$: Light that is scattered in Δz so that it leaves the new layer without reaching the original object.
3. $\mathbf{kS}$: Light that is scattered in Δz so that it passes into the original object, is scattered, and then is attenuated in Δz as it exits.
4. $\mathbf{Sk}$: Light that is attenuated in Δz, scattered by the object, and is then scattered by Δz such that it leaves the object.
5. $\mathbf{SkS}$: Light that is attenuated in Δz, scattered by the object, scattered in Δz back into the object, scattered again by the object, and then attenuated again.

Accounting for each of the five modes of scattering in turn, a new scattering function for $z+\Delta z$ can be written

$$\begin{aligned}\mathbf{S}(z+\Delta z) = \mathrm{e}^{-\sigma_t(\Delta z/\mu_i)}\mathrm{e}^{-\sigma_t(\Delta z/\mu_o)}\Bigg(&\mathbf{S}(z)+\\ &\mathbf{S}(z,z+\Delta z)+\mathbf{S}(z,z+\Delta z)\mathbf{S}(z)+\mathbf{S}(z)\mathbf{S}(z,z+\Delta z)+\\ &\mathbf{S}(z)\mathbf{S}(z,z+\Delta z)\mathbf{S}(z)+o(\Delta z^2)\Bigg),\end{aligned} \tag{3.2}$$

where $\mathbf{S}(z)$ is the scattering operator for a slab of thickness z and $\mathbf{S}(a,b)$ is the scattering operator for the portion of the slab from depth a to b.

We can simplify this further by replacing the $\mathrm{e}^{-c\Delta z}$ term with $1-c\Delta z+o(\Delta z^2)$ and taking advantage of an approximation to $\mathbf{S}$ for a layer that is infinitesimally thin [GY89]:

$$\mathbf{S}(z,z+\Delta z) = \mathbf{k}\Delta z + o(\Delta z^2).$$

Making these simplifications and then taking the difference between the new scattering operator $\mathbf{S}(z+\Delta z)$ and the scattering operator of the original layer $\mathbf{S}(z)$, we have

$$\begin{aligned}\mathbf{S}(z+\Delta z)-\mathbf{S}(z) = o(\Delta z^2)+\Bigg(&-\sigma_t(\frac{1}{\mu_i}+\frac{1}{\mu_o})\mathbf{S}(z)+\\ &\big(\mathbf{k}(z,z+\Delta z)+\mathbf{k}(z,z+\Delta z)\mathbf{S}(z)+\mathbf{S}(z)\mathbf{k}(z,z+\Delta z)+\\ &\mathbf{S}(z)\mathbf{k}(z,z+\Delta z)\mathbf{S}(z)\big)\Bigg)\Delta z\end{aligned}$$

Now we divide by Δz and take the limit as $\Delta z \to 0$, which gives us the infinitesimal change in the scattering function due to the addition of the new layer.

$$\frac{\partial \mathbf{S}}{\partial z} = -\sigma_t\left(\frac{1}{\mu_i}+\frac{1}{\mu_o}\right)\mathbf{S}+\big(\mathbf{k}+\mathbf{kS}+\mathbf{Sk}+\mathbf{SkS}\big) \tag{3.3}$$

We now need a boundary condition in order to convert this nonlinear integro-differential equation into an integral equation. If we assume that the object is bounded by a perfect absorber from below — *i.e.* $\mathrm{S}(0)=0$ — then application of the Laplace transform gives Equation 3.4. General boundary conditions are most easily handled with the adding equations; see the next section.

$$\begin{aligned}\mathbf{S}(z) = \int_0^z \mathrm{e}^{-\sigma_t(1/\mu_i+1/\mu_o)(z-z')}\big(&\mathbf{k}(z')+\mathbf{k}(z')\mathbf{S}(z')+\\ &\mathbf{S}(z')\mathbf{k}(z')+\mathbf{S}(z')\mathbf{k}(z')\mathbf{S}(z')\big)\,\mathrm{d}z'.\end{aligned} \tag{3.4}$$

We have written this with the operators expanded out; see Figure 4. This is a formidable equation, but like the rendering equation, it expresses a simple fact about light scattering. With computers and numerical methods, it can be solved. We will discuss previous solution techniques and some new Monte Carlo approaches for solving it in Section 4.

3.3 Adding equations

An important advantage of treating scattering functions directly is that it is possible to compute the combined scattering functions of aggregate objects from their individual scattering functions. These new scattering functions can be written directly in terms of the original ones and account for all scattering between the objects.

Consider two non-overlapping objects a and b with scattering functions $\mathbf{S}_a$ and $\mathbf{S}_b$. The scattering functions of the two objects together can be derived by considering all of the possible interactions between them. For example, consider the new scattering function for a pair of rays r_a and r'_a, both of which originate on a's boundary. Light may enter at a, be scattered by S_a, and then exit without interacting with b. This is the first term of Equation 3.6a. Or, it may be scattered in a so that it enters b, get scattered by b back into a, and then be scattered through a out to r_a; this gives the next term. By considering all such inter-reflections between a and b, we have the first adding equation [Pre65, Section 25].

$$\begin{aligned}\mathbf{S}_{a\to a} &= \mathbf{S}_a+\mathbf{S}_a\mathbf{S}_b\mathbf{S}_a+\mathbf{S}_a\mathbf{S}_b\mathbf{S}_a\mathbf{S}_b\mathbf{S}_a+\cdots && \text{(3.6a)}\\ &= \sum_{n=0}^{\infty}(\mathbf{S}_a\mathbf{S}_b)^n\mathbf{S}_a && \text{(3.6b)}\\ &= (\mathbf{I}-\mathbf{S}_a\mathbf{S}_b)^{-1}\mathbf{S}_a && \text{(3.6c)}\\ &= \mathbf{S}_a+\mathbf{S}_a\mathbf{S}_b\mathbf{S}_{a\to a}. && \text{(3.6d)}\end{aligned}$$

Given a ray r_a that enters a and another ray r_b that exits from b, we can derive a similar equation:

$$\begin{aligned}\mathbf{S}_{a\to b} &= \mathbf{S}_b\mathbf{S}_a+\mathbf{S}_b\mathbf{S}_a\mathbf{S}_b\mathbf{S}_a+\cdots && \text{(3.7a)}\\ &= \mathbf{S}_b\sum_{n=0}^{\infty}(\mathbf{S}_a\mathbf{S}_b)^n\mathbf{S}_a && \text{(3.7b)}\\ &= \mathbf{S}_b(\mathbf{I}-\mathbf{S}_a\mathbf{S}_b)^{-1}\mathbf{S}_a && \text{(3.7c)}\\ &= \mathbf{S}_b\mathbf{S}_a+\mathbf{S}_b\mathbf{S}_a\mathbf{S}_{a\to b}. && \text{(3.7d)}\end{aligned}$$

These equations are most easily understood by reading each term from right to left to see the order of scattering events.

Computing new scattering functions with the adding equations can be done much more efficiently than by recomputing the scattering functions of the aggregate object from scratch [van80]. This stems from the fact that $\mathbf{S}_a$ and $\mathbf{S}_b$ already incorporate all of the multiple scattering events inside a and b, so we need only to compute the effect of multiple scattering *between* the two objects. After a few terms, the series usually converges quickly, as long as not too much of the light is re-scattered at each step. Analysis based on the operator norm of each term could be used to describe the convergence more precisely. Since the results of this computation are new scattering functions, they can themselves be used in further computations of new scattering functions.

$$\mathrm{S}(z, r_i \to r_o) = \int_0^z \mathrm{e}^{-(\sigma_t(x_i)/\mu_i + \sigma_t(x_o)/\mu_o)(z-z')} \Bigg(\mathrm{k}(r_i(z') \to r_o(z')) + \frac{1}{4\pi} \int_{\mathcal{R}^+_{\mathcal{M}^2(z')}} \mathrm{k}(r_o \to -r')\, \mathrm{S}(z', r_i \to r') \frac{\mathrm{d}r'}{\mu^2_{r'}} +$$

$$\frac{1}{4\pi} \int_{\mathcal{R}^+_{\mathcal{M}^2(z')}} \mathrm{S}(z', r' \to r_o)\, \mathrm{k}(r_i \to r') \frac{\mathrm{d}r'}{\mu^2_{r'}} + \frac{1}{16\pi^2} \int_{\mathcal{R}^+_{\mathcal{M}^2(z')}} \int_{\mathcal{R}^+_{\mathcal{M}^2(z')}} \mathrm{S}(z', r'' \to r_o)\, \mathrm{k}(-r' \to -r'')\, \mathrm{S}(z', r_i \to r') \frac{\mathrm{d}r'}{\mu^2_{r'}} \frac{\mathrm{d}r''}{\mu^2_{r''}} \Bigg) \mathrm{d}z' \quad (3.5)$$

Figure 4: *The three dimensional integral scattering equation, 3.4, with operators expanded out and where the ray $r(t)$ is a new ray along the same line as r, constructed by offsetting the origin by distance t along the z axis and $x_i = x(r_i(z-z'))$ and $x_o = x(r_o(z-z'))$.*

3.4 One-dimensional setting

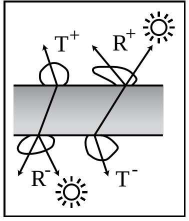

Figure 5: *The two reflection and transmission functions of a slab.*

There are useful special cases of the general scattering equation and the adding equations in the one-dimensional setting; this was where they were first derived. In one dimension, position in x and y is irrelevant, so the delta functions in the integral from the phase function disappear, leading to simpler formulas and easier implementation. A finite slab then has four scattering functions (see Figure 5): given illumination at the top, one gives the amount of light reflected at the top R^+ and another gives the amount of light transmitted at the bottom T^- [Cha60]. The other two, R^- and T^+, give reflection and transmission due to light incident at the bottom. R^+ and T^- are given in Equations 3.8 and 3.9, on the next page.

The application of the reflection and transmission operators to a function f is

$$(\mathbf{R} f)(\omega' \to \omega) = \frac{1}{4\pi} \frac{1}{\mu} \int_\Omega \mathrm{R}(\omega' \to \omega)\, f(\omega')\, \mathrm{d}\omega'$$

which gives us a nearly familiar equation for computing reflected radiance at a point:

$$\mathrm{L_o}(\omega) = \frac{1}{4\pi} \frac{1}{\mu} \int_\Omega \mathrm{R}(\omega' \to \omega)\, \mathrm{L_i}(\omega')\, \mathrm{d}\omega'$$

The reflection function of a surface is thus related to its BRDF f_r by $\mathrm{R}(\omega' \to \omega) = 4\pi f_\mathrm{r}(\omega' \to \omega)\mu'\mu$.

The adding equations are similarly simplified to integrals over just directions. In operator form, the scattering functions of two combined slabs a and b are

$$\begin{aligned}
\mathbf{R}^+_{a+b} &= \mathbf{R}^+_a + \mathbf{T}^+_a \mathbf{R}^+_b \mathbf{T}^-_a + \mathbf{T}^+_a \mathbf{R}^+_b \mathbf{R}^-_a \mathbf{R}^+_b \mathbf{T}^-_a + \cdots \\
\mathbf{R}^-_{a+b} &= \mathbf{R}^-_b + \mathbf{T}^-_b \mathbf{R}^-_a \mathbf{T}^+_b + \mathbf{T}^-_b \mathbf{R}^-_a \mathbf{R}^+_b \mathbf{R}^-_a \mathbf{T}^+_b + \cdots \\
\mathbf{T}^-_{a+b} &= \mathbf{T}^-_b \mathbf{T}^-_a + \mathbf{T}^-_b \mathbf{R}^-_a \mathbf{R}^+_b \mathbf{T}^-_a + \cdots \\
\mathbf{T}^+_{a+b} &= \mathbf{T}^+_a \mathbf{T}^+_b + \mathbf{T}^+_a \mathbf{R}^+_b \mathbf{R}^-_a \mathbf{T}^+_b + \cdots
\end{aligned}$$

3.5 Discussion

The scattering equations thus bring us to a new framework for considering rendering problems. Note that there are no fundamentally new types of rendering problems that the scattering equations make accessible: as noted in Section 2.3, the formal inverse of the operator rendering equation can be used to solve the same kinds of scattering problems as well. For example, Hanrahan and Krueger effectively used a Neumman series expansion of the inverse to estimate four-dimensional scattering functions. This method could be easily extended to higher-dimensional scattering problems, and more sophisticated Monte Carlo techniques could be applied.

Conversely, the scattering equation can be used for more than just pre-computing scattering functions. Given knowledge of particular viewing conditions, particular lighting conditions, or both, we can directly compute estimates of integrals such as $\mathbf{S}\mathrm{L}_e$ (where L_e is emitted radiance), rather than first computing $\mathbf{S}$ and then passing emitted light through it. Since both approaches are based on formulae that directly describe the physics of light scattering, it is not surprising that the two approaches are connected in this way. In fact (and reassuringly), the scattering equation can be derived directly from the equation of transfer [Pre65].

In the next section, we will see that solving the scattering equation involves sampling chains of scattering events through a medium and evaluating their contribution—precisely how the equation of transfer is typically solved. Considered in light of its connections with the equation of transfer, we can use the scattering equation as a path to insights about how to solve the equation of transfer, and vice versa. This has the potential to lead to new ways of considering some classic rendering problems.

4 Monte Carlo Solution

A previously uninvestigated technique for solving the scattering and adding equations is Monte Carlo integration. Monte Carlo is a particularly effective technique for solving high dimensional integrals and integrals with discontinuities in the integrand. Its generality makes it possible to compute integrals where the functions in the integrand vary almost arbitrarily [KW86]; here, it allows wide variety in the possible phase functions, scattering and attenuation coefficients, and geometric shapes.

Techniques previously used to solve the scattering and adding equations have been based on the integro-differential form such as Equation 3.3. Typically, the set of angles is discretized and a system of non-linear differential equations is solved to compute scattering at the discrete angles (Max *et al.* took this approach). See van de Hulst [van80] for a survey and comparison of many of the variations of these techniques. These methods all break down in the face of complexity in the scattering medium: given highly anisotropic phase functions or non-homogeneous media, they are either not applicable due to the assumptions made in their derivations, or become increasingly inefficient because finer discretizations are required and the systems of equations become large. Furthermore, the generalization of these methods to higher-dimensional settings quickly becomes intractable, which has stymied the development of the more general theory.

4.1 Random walk solution

We will describe a simple recursive solution of the integral scattering equation. Because $\mathbf{S}(z)$ in Equation 3.4 is written recursively in terms of integrals of scattering functions of $\mathbf{S}(z')$, we can evaluate an estimate of $\mathbf{S}(z)$ based on a random walk. (The spirit of this algorithm is similar to Kajiya's path tracing solution to the rendering equation.) We follow a two step process:

1. First we sample the integral over depth by choosing z', where $0 < z' < z$. For constant attenuation functions, the exponential term can be importance sampled directly: to sample the integral $\int_0^z \mathrm{e}^{az'} \mathrm{d}z'$, where $a = -\sigma_t(1/\mu_i + 1/\mu_o)$, we first find the

$$\mathrm{R}^{+}(z,\omega_i \to \omega_o) = \int_0^z \mathrm{e}^{-\sigma_t(z')(1/\mu_i+1/\mu_o)(z-z')}\,\sigma_s(z')\Bigg(\mathrm{p}(z',\omega_i \to \omega_o) + \frac{1}{4\pi}\int_\Omega \mathrm{p}(z',-\omega' \to \omega_o)\,\mathrm{R}^{+}(z',\omega_i \to \omega')\,\frac{\mathrm{d}\omega'}{\mu'} +$$

$$\frac{1}{4\pi}\int_\Omega \mathrm{R}^{+}(z',\omega' \to \omega_o)\,\mathrm{p}(z',\omega_i \to -\omega')\,\frac{\mathrm{d}\omega'}{\mu'} + \frac{1}{16\pi^2}\int_\Omega\int_\Omega \mathrm{R}^{+}(z',\omega'' \to \omega_o)\,\mathrm{p}(z',-\omega' \to -\omega'')\,\mathrm{R}^{+}(z',\omega_i \to \omega')\,\frac{\mathrm{d}\omega'\mathrm{d}\omega''}{\mu'\mu''}\Bigg)\mathrm{d}z' \qquad (3.8)$$

$$\mathrm{T}^{-}(z,\omega_i \to \omega_o) = \delta(\mu_i - \mu_o)\mathrm{e}^{-\int_0^z \sigma_t(z')\mathrm{d}z'/\mu_i} + \int_0^z \mathrm{e}^{-\sigma_t(z)(z-z')/\mu_i}\,\sigma_s(z')\Bigg(\mathrm{e}^{-z'/\mu_o}\mathrm{p}(z',\omega_i \to -\omega_o) +$$

$$\mathrm{e}^{-z'/\mu_o}\frac{1}{4\pi}\int_\Omega \mathrm{p}(z',-\omega' \to \omega_o)\,\mathrm{R}^{+}(z,\omega_i \to \omega')\,\frac{\mathrm{d}\omega'}{\mu'} + \frac{1}{4\pi}\int_\Omega \mathrm{T}^{-}(z',\omega' \to \omega_o)\,\mathrm{p}(z',\omega_i \to -\omega')\,\frac{\mathrm{d}\omega'}{\mu'} +$$

$$\frac{1}{16\pi^2}\int_\Omega\int_\Omega \mathrm{T}^{-}(z',\omega'' \to \omega_o)\,\mathrm{p}(z',-\omega' \to -\omega'')\,\mathrm{R}^{+}(z',\omega_i \to \omega')\,\frac{\mathrm{d}\omega'\mathrm{d}\omega''}{\mu'\mu''}\Bigg)\mathrm{d}z' \qquad (3.9)$$

Figure 6: *The integral forms of the one-dimensional reflection and transmission equations. Since the medium is assumed to be homogeneous in x and y and that incident illumination is constant over a large area relative to σ_t, the equations are expressed in terms of depths and a pair of directions, rather than all of ray space. Note that an additional term is added to* T *to account for directly transmitted light.*

probability density function $\mathrm{pdf}(z') = \frac{a\mathrm{e}^{az'}}{\mathrm{e}^{az}-1}$. The cumulative distribution function $P(z)$ is $\int_0^z \mathrm{pdf}(z')\mathrm{d}z'$. Given a random number ξ between 0 and 1, we set $\xi = P(z')$ and solve for z':

$$z' = \frac{\log(1+\xi(\mathrm{e}^{az}-1))}{a}.$$

More generally, if the attenuation term varies with depth, the pdf cannot be computed analytically. In this case, we sample an optical thickness and march through the medium until that distance has been covered. In either case, the resulting sample is weighted by the exponential term at z' divided by the pdf.

2. We compute the product of the weight and estimates of the terms $\mathbf{k}(z') + \mathbf{k}(z')\mathbf{S}(z') + \mathbf{S}(z')\mathbf{k}(z') + \mathbf{S}(z')\mathbf{k}(z')\mathbf{S}(z')$. In computing the terms, we will come to have new estimates of the scattering equation $\mathbf{S}$ to compute; we proceed recursively.

This process is most easily understood in the one-dimensional case (Equation 3.8). Figure 7 gives pseudo-code for evaluating the 1D reflection function.

There is an important difference between this process and random walk solutions of the equation of transfer: as the recursion continues, the z' at which we are estimating $\mathbf{S}$ is monotonically decreasing. Once we have chosen a depth at which to estimate $\mathbf{S}$, all scattering above z' is irrelevant; it has already been accounted for. In effect, we are able to make a single pass through the medium from top to bottom, peeling off layers and solving scattering problems for thinner sub-objects. In comparison, standard approaches to solving the equation of transfer do not create a progressively simpler problem as they proceed.

4.2 Three-dimensional case

In the 3D case, this sampling process is less straightforward due to the delta function in the ray space phase function. Fortunately, delta functions generally fit easily into Monte Carlo sampling schemes. For example, given two rays r and r', the $\mathbf{k}(z')$ term of Equation 3.4 is zero unless both r and r' start at the same point *and* the z' depth sampled in step 1 above matches that point. In general two rays in 3D do not meet at all. Therefore, in the process of sampling the integrals, whenever we have a choice of rays to sample, sometimes we must carefully choose a ray and a depth such that this delta function is non-zero. To make this easier, we separate $\mathbf{S}$ into two components, $\mathbf{S}_\mathrm{s}$, scattering due to a single scattering event, and $\mathbf{S}_\mathrm{m}$, scattering due to multiple scattering events. This is analogous to distribution ray tracing with a mixed pure specular and diffuse surface where the two parts need to be sampled separately. $\mathbf{S}_\mathrm{s}(z) = \int_0^z \mathrm{e}^{\cdots}\mathbf{k}\,\mathrm{d}z'$ and $\mathbf{S}_\mathrm{m}(z) = \int_0^z \mathrm{e}^{\cdots}(\mathbf{kS}+\mathbf{Sk}+\mathbf{SkS})\,\mathrm{d}z'$. Thus, $\mathbf{S} = \mathbf{S}_\mathrm{s} + \mathbf{S}_\mathrm{m}$.

Consider the specific case of estimating $\mathrm{L}_\mathrm{o} = \mathbf{S}\mathrm{L}_e$ for a given outgoing ray r and a single point light source. Separating $\mathbf{S}$, we have two integrals, $\mathbf{S}_\mathrm{s}\mathrm{L}_e + \mathbf{S}_\mathrm{m}\mathrm{L}_e$. The first term is easily handled: it just represents single scattering of emitted light in the medium, so all scattering events are along r's path through the object. We choose positions for scattering events (*i.e.* x' in Figure 8a) by importance sampling points along r as above. Given these points, the incoming ray r' follows directly since the light is a point source; for an area light, a point can be chosen on the source and r then follows.

Moving on to $\mathbf{S}_\mathrm{m}\mathrm{L}_e$, and in particular the term, $\mathbf{Sk}\mathrm{L}_e = \mathbf{S}_\mathrm{s}\mathbf{k}\mathrm{L}_e + \mathbf{S}_\mathrm{m}\mathbf{k}\mathrm{L}_e$ (treatment of $\mathbf{kS}$ is analogous). We first randomly sample a point x' on the surface where the $\mathbf{k}$ scattering event happens, using an exponential distribution centered around $x(r)$ (Figure 8b). This strategy is based on the assumption that the longer the distance light travels under the surface, the more it will be attenuated and the less impact it will have. This defines a ray r' to the light due to the point light assumption (as above, area lights are a straightforward extension). The second single scattering event must be along r's path through the medium and must have a direction such that it passes through $x(r')$ in order for all of the respective delta functions to be non-zero. We therefore chose a depth along r with importance sampling.

There is more freedom in sampling from the $\mathbf{S}_\mathrm{m}\mathbf{k}\mathrm{L}_e$ term (Figure 8c). We choose a ray r' as above, and still must have the $\mathbf{k}$ scattering event at $x(r')$ for the delta function in $\mathbf{k}$ to be non-zero. However, the direction of r'' can be chosen arbitrarily since $\mathbf{S}_\mathrm{m}$ doesn't have the delta function along the path of r through the medium that $\mathbf{S}_\mathrm{s}$ does. We simply importance sample the phase function based on $\omega(r')$ to get the ray direction for the r''.

Finally, the $\mathbf{SkS}\mathrm{L}_e$ term is slightly different: we also need to choose two rays that meet at a point where the $\mathbf{k}$ term will be evaluated (Figure 8d). We sample the shared ray origin from an exponential distribution centered around the midpoint between $x(r)$ and $x(r')$. Given this origin that the two new rays share, we again use importance sampling with the phase function to choose the two ray directions.

4.3 Solving the adding equations

Monte Carlo estimation of the adding equations introduces two issues: how many terms to evaluate of the infinite sum of products of scattering functions, and how to estimate individual terms of the sum. We solve the first problem and compute an unbiased estimate of the infinite sum by probabilistically terminating the series; after

```
**Procedure** R($z$, $\omega_i$, $\omega_o$) $\equiv$
    ($z'$, *pdf*) := sampleDepth($\sigma_t$, $z$)
    *scale* := $e^{-(z-z')*\sigma_t*(\frac{1}{\mu_i}+\frac{1}{\mu_o})}$ / *pdf*
    *result* := $\sigma_s$ * p($\omega_i$, $\omega_o$)
    **if** (**not** terminate()) **then**
        ($\omega'$, *pdf'*) := sampleAngle($p$, $\omega_o$)
        *result* := *result* + $\sigma_s$ * p(-$\omega'$, $\omega_o$) * R($z'$, $\omega_i$, $\omega'$) /
                ($\cos\omega'$ * *pdf'*)
        ($\omega''$, *pdf''*) := sampleAngle($p$, $\omega_i$)
        *result* := *result* + R($z'$, $\omega''$, $\omega_o$) * $\sigma_s$ * p($\omega_i$, -$\omega''$) /
                ($\cos\omega'$ * *pdf''*)
        *result* := *result* + R($z'$, $\omega'$, $\omega_o$) * $\sigma_s$ * p(-$\omega''$, -$\omega'$) *
                R($z'$, $\omega_i$, $\omega''$) / ($\cos\omega'$ * $\cos\omega''$ * *pdf'* * *pdf''*)
    **endif**
    **return** *result* * *scale*
```

Figure 7: *Pseudo-code for evaluation of the one-dimensional reflection equation. The phase function* p(), σ_s*, and* σ_t *are all potentially varying with depth. The* terminate() *function probabilistically stops the recursion using Russian roulette based on the weighted contribution that this estimate of* R *will make to the final solution. The* sampleAngle() *function uses importance sampling to choose an outgoing angle based on the phase function and the incoming angle; it returns the new direction and its probability density.*

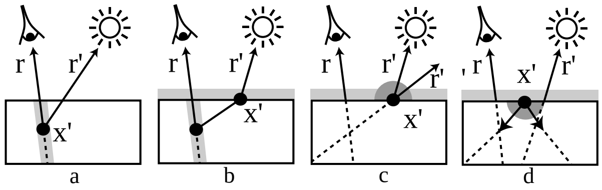

Figure 8: *Sampling rays* r' *in the 3D case; hilighted regions denote terms that are free to be sampled. From left to right: for direct lighting, all scattering events are along r's path through the medium; for* $\mathbf{S}_s$*, we sample a distance along r to find a scattering event—this gives a ray that connects through the point* x' *on the boundary; for* $\mathbf{S}_m$*, we have more freedom to sample the direction of* r'' *and can use a variety of importance functions; finally, for* **SkS***, we sample a point for the scattering event* **k** *and then sample the two outgoing directions.*

computing estimates of the first few terms, we terminate with some probability after each successive term. When we continue on, subsequent terms until we do terminate are multiplied by a correction factor so that the final result is unbiased [AK90].

Given a particular term of the form of Equation 3.1, we have the multiple integral represented by the composition of a set of scattering functions to estimate. Given an incident and a reflected ray, we need to sample a set of rays r_i that connect the two of them together. These can be sampled in any order—the key is to find chains of rays where the scattering functions make a large contribution; this is the same problem faced in light transport problems [Vea97].

We have implemented routines that solve the 1D adding equations. We have implemented them in a modular fashion: they are given abstract data types describing the top and bottom layers as well as the incoming and outgoing directions. The layer objects provide a small number of operations to the adding routines. They are: evaluation given two angles, importance sampling one direction given the other (for layers where distributions for importance sampling are not easily computed, a default implementation uniformly samples the hemisphere), returning the probability density function of sampling one direction given the other direction (this is useful for multiple importance sampling), and a boolean function which tells if its scattering functions are delta functions (see below). These operations make it possible to implement a variety of representations for layers and easily add them together.[3]

Delta functions may be present in this series due to direct transmission (Equation 3.9) as well due to layers that specularly reflect or refract light (*e.g.* a mirror reflector at the bottom, or a Fresnel layer at the top). These are tricky because the delta functions cannot be evaluated, but only sampled—the evaluation routines always return zero. However, when such a layer samples a new direction given an incident or outgoing direction, it can pick the appropriate scattered direction. For example, when computing the term $T^+R^+T^-$ when the top layer is a Fresnel reflector, we compute both the incident and outgoing directions to the bottom layer by sampling T^+ and T^- given the outgoing and incident directions at the top, respectively; the reflection function R^+ has no choice in sampling its incident and outgoing directions, as it would never be able to randomly find an outgoing direction that is transmitted into the final outgoing direction.

5 Results

In this section, we start by demonstrating the efficiency of the scattering equations for solving rendering problems. We then demonstrate the use of the 1D scattering and adding equations to rendering complex surfaces and show applications of the 3D scattering equation to accurate rendering of surfaces, accounting for light that enters the surface some distance from where it exits.

5.1 Accuracy and efficiency

We tested our implementation's accuracy against a model that corresponds to the standard problem in astrophysics. This model is specified by the atmosphere's optical thickness, albedo, and phase function. The resulting scattering functions have been computed and tabularized by many authors. We compared our results to tables from Bellman *et al.* [BKP63], which have results computed by using Gaussian quadrature to generate a system of differential equations which were then solved via the Runge-Kutta method.

For a set of roughly forty randomly-selected albedos, thicknesses, and pairs of angles, we found excellent agreement with the scattering function values our routines computed. We have also verified our implementation of the adding equations by comparing the scattering function values computed by applying the adding equations to two halves of an object to those computed directly for the aggregate. Finally, we verified that our 3D implementation gave the same results as the 1D equation for uniformly illuminated planar objects that have homogeneous scattering properties in *xy*.

We then conducted a series of experiments to compare the efficiency of our solution method to a standard solution method that uses the equation of transfer. We implemented a Monte Carlo sampling routine that uses the equation of transfer to estimate the scattering function of a medium for a pair of angles based on a random walk. Our implementation is similar to the algorithm described by Hanrahan and Krueger [HK93]: a particle is injected into the medium from the incident direction and followed along a path through the medium. The walk is biased so that at each scattering event, the attenuation to the surface in the outgoing direction is computed and the result is accumulated to estimate the function's value. Russian roulette is used to terminate this process, based on the accumulated weight of the path.

[3] See Pharr and Veach for applications of similar abstractions to combining procedural shading with physically based rendering [PV00].

After verifying that both methods converged to the same results, we compared their relative efficiency. For a variety of thicknesses, scattering coefficients, absorption coefficients, and phase functions, we computed accurate estimates of the scattering function for a pair of angles. We used a phase function due to Henyey and Greenstein [HG41]; it takes an asymmetry parameter, g that is the average value of the product of the phase function with the cosine of the angle between ω' and ω. The range of g is from -1 to 1, corresponding to total back-scattering to total forward scattering, respectively. We then applied both solution methods to computing estimates of the scattering functions for the pair of angles, giving each the same amount of processor time. The same Russian roulette termination parameters were used for each method and importance sampling was applied in analogous places (*e.g.* for sampling the outgoing direction of the phase function at scattering events for the equation of transfer). Our implementation generally computed five to ten estimates with the equation of transfer in the time it took to compute one estimate with the scattering equation.

The graphs in Figure 9 show some of the results. We computed the ratio of variance of the equation of transfer solution to the scattering equation solution, after giving each the same amount of processor time. The scattering equation solution often had 5 to 10 times less variance, though for some configurations (strongly anisotropic phase functions and very thick objects), it sometimes had over 100 times less variance. Although the scattering equation generally performed quite well, for cases with high albedos the equation of transfer was sometimes more efficient. We believe that this is due to our recursive sampling process: because we compute a geometrically-increasing number of recursive estimates of R^+ at each level of recursion, it is possible to end up computing a large number of estimates that have a relatively little influence on the final result. The scattering equation also did well for most phase function parameters, except for extreme backward scattering. In this case, although most of incident light is quickly scattered back out of the top, we still continue to work through the z depth of the medium, not allocating effort as well as we might.

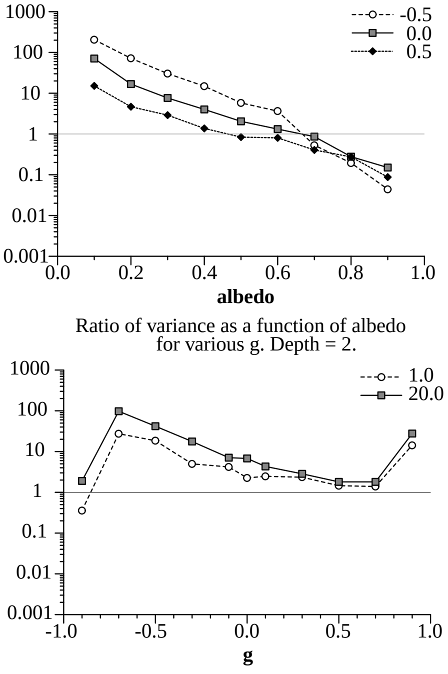

Ratio of variance as a function of albedo
for various g. Depth = 2.

Ratio of variance as a function of g
for various depths. Albedo = 0.4

Figure 9: *Comparing our solutions of the "standard problem." After giving each method the same amount of processor time to compute the best possible solution, we have graphed the ratio of variance when the equation of transfer is sampled to the variance when the scattering equation is sampled. Points above 1 on the y axis indicate situations where the scattering equation is more efficient. Because both sampling methods converge at the same rate asymptotically, the ratio of running time to compute solutions of equivalent quality is proportional to the variance ratio.*

5.2 Scattering from surfaces

To illustrate the use of the 1D adding and scattering equations for rendering, we took a dragon model with a standard specular and diffuse shading model and added scattering layers to it, using the adding equations to compute the new scattering function that describes the composition of the base surface layer with the new scattering layer. As such, the result is an accurate simulation of subsurface light transport. When the routines that compute the adding equations needed to evaluate the reflection or transmission functions of the added layer, a new Monte Carlo estimate for that pair of angles was computed. With a not-very-optimized implementation, the images each took a few minutes to render on a modern PC.

The series of images in Figure 10 shows the results. The first image shows the object shaded with the standard shading model. As the thickness of the new layer increases going from left to right, the shiny copper base surface is gradually overwhelmed by the grey and more diffuse added layer. Eventually just a shadow of the specular highlights is left and finally no trace of the base surface once the new layer is sufficiently thick. Notice that the silhouette edges are affected more strongly by the added layer; this is because the rays traveling at oblique angles go a longer distance through the new layer. The rightmost image shows the result of procedurally varying the thickness of the added layer based on the local surface normal in an effort to simulate scattering effects of dust (modeled in a manner similar to Hsu and Wong [HW95]).

5.3 Scattering from volumes

As a final example, we generated some images to demonstrate the use of the 3D scattering equation to compute reflection from complex surfaces and performed some experiments to understand the properties of subsurface light transport.

To determine how distance from the point of illumination affected the intensity of reflected light, we illuminated half of a slab from the direction along its normal and looked at the scattering function's magnitude in the normal direction at a series of points moving away from the illuminated area. Figure 11 shows the results. As one might expect, reflectance drops off roughly exponentially. Other experiments showed that as the object gets thinner, light entering from far away becomes less important, because more light scatters out of the object before traveling very far. These observations help validate some of the assumptions made in designing importance sampling techniques for 3D scattering equation.

Inspired by the images of Dorsey *et al.*, we rendered some images of marble, in the form of a marble block. Scattering properties were computed procedurally using noise functions [Per85]. Figure 12 shows a comparison of rendering a block with the 1D scattering equation (left) compared to a rendering with the 3D scattering equation (right). The right halves of the blocks were brightly illuminated by a directional light source, while the left halves were lit dimly. There are a number of significant differences between the two images. Most strikingly, when subsurface light transport is accounted for we can see the effect of light that entered in the illuminated half and then scattered into the unilluminated half. Furthermore, the veins of the marble, where the attenuation coefficient is high, cast shadows inside the volume; this effect is missing in the 1D case. A subtle difference between the two can be seen along

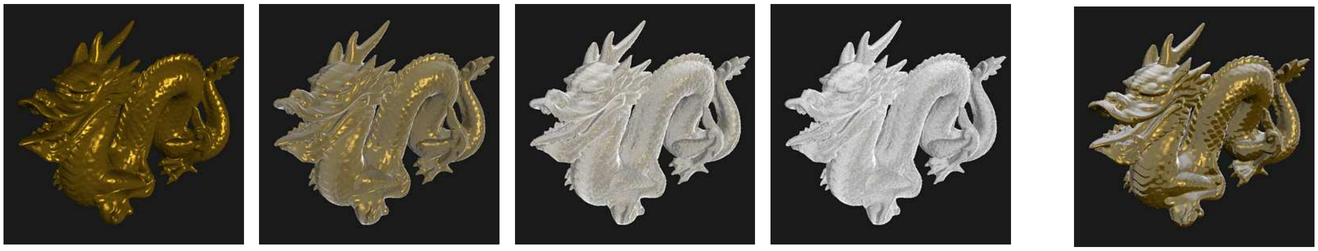

depth = 0. depth = 0.2 depth = 0.8 depth = 2.0

Figure 10: *Adding layers to a model; thicknesses are increasing from left to right. On the right, the thickness is determined procedurally to simulate dust. For all images,* $\sigma_s = 0.5$, $\sigma_a = 0.5$, $g = -0.15$. *Because the adding equations and scattering equations are used to compute the aggregate scattering function, the results accurately account for all inter-reflection inside the added layer as well as between the layer and the base surface.*

the edges: they are more transparent in the 3D version, since the geometry of the object is accounted for in computing subsurface scattering and rays leave the object after a short distance.

6 Summary and Conclusion

In this paper we have introduced a new theoretical framework for light scattering to computer graphics. This theory has scattering as its basic foundation, rather than light transport. We have applied the theory to rendering subsurface scattering from complex objects using Monte Carlo integration. For some rendering problems (and with the sampling algorithms we used), the scattering equation can be solved more efficiently than the equation of transfer. The adding equations exhibit efficiencies by providing a way to break rendering problems into smaller parts and then reassemble the partial solutions; this gives a theoretical basis to clustering algorithms and a new way to apply clustering to Monte Carlo rendering algorithms.

Part of the advantage from the scattering equation solution stems from the fact that its recursive expansion has a bidirectional effect—paths are constructed in both directions and meet in the middle. Our sampling of the **SkS** term reflects a *non-local* sampling strategy [Vea97], where a scattering event at **k** is chosen before either of its adjacent scattering events have been sampled. This is in contrast to previous bidirectional sampling strategies that incrementally build paths by finding new vertices directly from a previous vertex. As such, understanding the connections between the path sampling strategies that we have used and previous bidirectional path sampling strategies is important future work. In particular, techniques that ameliorate the exponential nature of the recursive sampling and more effectively re-use sub-paths should improve performance in cases where the albedo is high. Another area for further investigation is better importance sampling techniques for the 3D case and the application of multiple importance sampling to reduce variance.

Our example of subsurface scattering as a demonstration of the three-dimensional scattering equation reflects a choice in scale rather than limitation of theory. The scattering and adding equations have applications to computing scattering from complex volumetric objects at larger scales, such as clouds, smoke, sunbeams, *etc*. As such, this approach has applications to the level-of-detail problem. The 3D scattering and adding equations provide the correct mathematical setting for two of the outstanding problems in level-of-detail identified by Kajiya and Kay [KK89]: automatic computation of texels from complex geometry, and computation of aggregate texels that represent two nearby texels. Furthermore, scattering functions are the correct abstraction to use to replace geometry; techniques based on BRDFs (*e.g.* [Kaj85, Ney98]) are inaccurate in that they do not correctly incorporate the effect of light that enters an object at a different place than it exits.

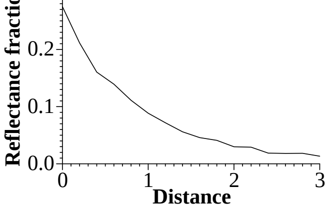

Figure 11: *Reflection function magnitude in the unilluminated part of an object as a function of distance from the boundary of illuminated region.* $\sigma_a = 0.5$, $\sigma_s = 0.5$, $g = 0$.

This theory has applications to many classic problems in rendering, including replacing geometry with scattering functions and efficiently re-rendering scenes with changes in illumination or as objects are added to or removed from them. Equally important, it has promise as a way to suggest new sampling strategies for solving the rendering equation more effectively. Understanding the connections between solution techniques that have previously been used for each of these approaches gives many directions for future work.

Acknowledgements

Discussions with Eric Veach about this work and about connections with bidirectional light transport algorithms in particular were very useful. Thanks also to the reviewers for insightful comments. The dragon model was provided by the Stanford 3D Scanning Repository. Matt Pharr was supported by a Pixar Animation Studios graduate fellowship, DARPA contract DABT63-95-C-0085 and NSF contract CCR-9508579.

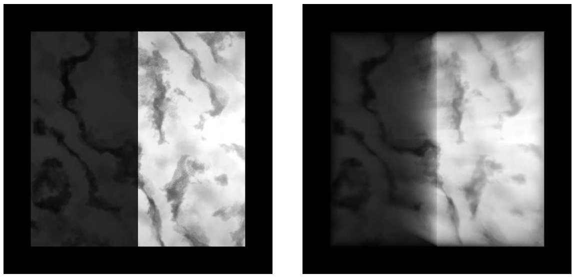

Figure 12: *Comparison of rendering subsurface scattering from a side-lit marble cube with the 1D scattering equation (left) and the 3D scattering equation (right). Since the 3D solution considers light that enters the surface away from where it exits, subsurface light transport is more accurately modeled.*

References

[AK90] James Arvo and David Kirk, *Particle transport and image synthesis*, Computer Graphics **24** (1990), no. 4, 63–66.

[Amb42] V. A. Ambarzumian, *A new method for computing light scattering in turbid media*, Izv. Akad. Nauk SSSR **3** (1942).

[Amb58] V. A. Ambarzumian (ed.), *Theoretical astrophysics*, Pergamon Press, New York, New York, 1958.

[BK56] Richard Bellman and Robert Kalaba, *On the principle of invairant imbedding and propagation through inhomoheneous media*, Proceedings of the National Academy of Sciences **42** (1956), 629–632.

[BKP63] Richard E. Bellman, Robert E. Kalaba, and Marcia C. Prestrud, *Invariant imbedding and radiative transfer in slabs of finite thickness*, American Elsevier Publishing Company, New York, 1963.

[Bli82] James F. Blinn, *Light reflection functions for simulation of clouds and dusty surfaces*, Computer Graphics **16** (1982), no. 3, 21–29.

[BW75] Richard E. Bellman and G. M. Wing, *An introduction to invariant imbedding*, John Wiley & Sons, New York, 1975.

[Cha60] S. Chandrasekar, *Radiative transfer*, Dover Publications, New York, 1960, Originally published by Oxford University Press, 1950.

[DEL^{+}99] Julie Dorsey, Alan Edelman, Justin Legakis, Henrik Wann Jensen, and Hans Køhling Pedersen, *Modeling and rendering of weathered stone*, Proceedings of SIGGRAPH 99 (August 1999), 225–234.

[GY89] R. M. Goody and Y. L. Yung, *Atmospheric radiation*, Oxford University Press, 1989.

[HG41] L. G. Henyey and J. L. Greenstein, *Diffuse radiation in the galaxy*, Astrophysical Journal **93** (1941), 70–83.

[HK93] Pat Hanrahan and Wolfgang Krueger, *Reflection from layered surfaces due to subsurface scattering*, Computer Graphics Proceedings, August 1993, pp. 165–174.

[HM92] Chet S. Haase and Gary W. Meyer, *Modeling pigmented materials for realistic image synthesis*, ACM Transactions on Graphics **11** (1992), no. 4, 305–335.

[HW95] Siu-Chi Hsu and Tien-Tsin Wong, *Simulating dust accumulation*, IEEE Computer Graphics and Applications **15** (1995), no. 1, 18–25.

[Kaj85] James T. Kajiya, *Anisotropic reflection models*, Computer Graphics (SIGGRAPH '85 Proceedings), vol. 19, July 1985, pp. 15–21.

[Kaj86] James T. Kajiya, *The rendering equation*, Computer Graphics **20** (1986), no. 4, 143–150.

[KK89] James T. Kajiya and Timothy L. Kay, *Rendering fur with three dimensional textures*, Computer Graphics **23** (1989), no. 3, 271–280.

[KM31] P. Kubelka and F. Munk, *Ein Beitrag zur Optik der Farbanstriche*, Z. Tech. Physik. **12** (1931), 593.

[KW86] Malvin H. Kalos and Paula A. Whitlock, *Monte Carlo methods: Volume I: Basics*, John Wiley & Sons, New York, 1986.

[Laf96] Eric Lafortune, *Mathematical models and Monte Carlo algorithms for physically based rendering*, Ph.D. thesis, Katholieke Universiteit Leuven, February 1996.

[LW94] Eric Lafortune and Yves Willems, *A theoretical framework for physically based rendering*, Computer Graphics Forum **13** (1994), no. 2, 97–107.

[MM98] Gavin Miller and Marc Mondesir, *Rendering hyper-sprites in real time*, Eurographics Rendering Workshop 1998 (1998), 193–198.

[MMKW97] Nelson Max, Curtis Mobley, Brett Keating, and En-Hua Wu, *Plane-parallel radiance transport for global illumination in vegetation*, Eurographics Rendering Workshop 1997, Eurographics, Springer Wien, June 1997, pp. 239–250.

[Mob94] Curtis D. Mobley, *Light and water: Radiative transfer in natural waters*, Academic Press, 1994.

[Ney98] Fabrice Neyret, *Modeling, animating, and rendering complex scenes using volumetric textures*, IEEE Transactions on Visualization and Computer Graphics **4** (1998), no. 1.

[NRH^{+}77] Fred E. Nicodemus, J. C. Richmond, J. J. Hisa, I. W. Ginsberg, and T. Limperis, *Geometrical considerations and nomenclature for reflectance*, Monograph number 160, National Bureau of Standards, Washington DC, 1977.

[NUW98] H. H. Natsuyama, S. Ueno, and A. P. Wang, *Terrestial radiative transfer*, Springer-Verlag, Hong Kong, 1998.

[Per85] Ken Perlin, *An image synthesizer*, Computer Graphics (SIGGRAPH '85 Proceedings), vol. 19, July 1985, pp. 287–296.

[PP51] Glenn H. Peebles and Milton S. Plesset, *Transmission of gamma-rays through large thicknesses of heavy materials*, Physical Review **81** (1951), no. 3, 430–439.

[Pre58] Rudolph W. Preisendorfer, *Invariant imbedding relation for the principles of invariance*, Proceedings of the National Academy of Sciences **44** (1958), 320–323.

[Pre65] Rudolph W. Preisendorfer, *Radiative transfer on discrete spaces*, Pergamon Press, Oxford, 1965.

[Pre76] R. W. Preisendorfer, *Hydrologic optics*, U.S. Department of Commerce, National Oceanic and Atmospheric Administration, Honolulu, Hawaii, 1976, Six volumes.

[PV00] Matt Pharr and Eric Veach, *Shading with closures*, In preparation, 2000.

[RPV93] Holly Rushmeier, Charles Patterson, and Aravindan Veerasamy, *Geometric simplification for indirect illumination calculations*, Proceedings of Graphics Interface '93, May 1993, pp. 227–236.

[SD95] François Sillion and George Drettakis, *Feature-based control of visibility error: A multi-resolution clustering algorithm for global illumination*, SIGGRAPH 95 Conference Proceedings, Addison Wesley, August 1995, pp. 145–152.

[SDS95] François Sillion, G. Drettakis, and Cyril Soler, *A clustering algorithm for radiance calculation in general environments*, Eurographics Rendering Workshop 1995, Eurographics, June 1995.

[Sto62] George Stokes, *On the intensity of the light reflected from or transmitted through a pile of plates*, Proceedings of the Royal Society (1862), Reprinted in Mathematical and Physical Papers of Sir George Stokes, Volume IV, Cambridge, 1904.

[TJH66] S. Twomey, H. Jacobowitz, and H. B. Howell, *Matrix methods for multiple-scattering problems*, Journal of the Atmospheric Sciences **23** (1966), 289–296.

[TS67] K. E. Torrance and E. M. Sparrow, *Theory for off-specular reflection from roughened surfaces*, Journal of the Optical Society of America **57** (1967), no. 9.

[van80] Hendrik Christoffel van de Hulst, *Multiple light scattering*, Academic Press, New York, 1980, Two volumes.

[Vea97] Eric Veach, *Robust Monte Carlo methods for light transport simulation*, Ph.D. thesis, Stanford University, December 1997.

[VG94] Eric Veach and Leonidas Guibas, *Bidirectional estimators for light transport*, Fifth Eurographics Workshop on Rendering (Darmstadt, Germany), June 1994, pp. 147–162.

[VG95] Eric Veach and Leonidas J. Guibas, *Optimally combining sampling techniques for Monte Carlo rendering*, Computer Graphics Proceedings, August 1995, pp. 419–428.

[Wan90] Alan P. Wang, *Basic equations of three-dimensional radiative transfer*, Journal of Mathematical Physics **31** (1990), no. 1, 175–181.

[WAT92] Stephen Westin, James Arvo, and Kenneth Torrance, *Predicting reflectance functions from complex surfaces*, Computer Graphics **26** (1992), no. 2, 255–264.

[ZWCS99] Douglas E. Zongker, Dawn M. Werner, Brian Curless, and David H. Salesin, *Environment matting and compositing*, SIGGRAPH 99 Conference Proceedings, Addison Wesley, August 1999, pp. 205–214.